Original Article

Magnetic resonance cholangiopancreatography at 3T in a single breath-hold: comparative effectiveness between three-dimensional (3D) gradient- and spin-echo and two-dimensional (2D) thick-slab fast spin-echo acquisitions

Cheng-Ping Chien[1,2], Feng-Mao Chiu[3], Yen-Chun Shen[2], Yi-Hsun Chen[2], Hsiao-Wen Chung[1]

[1]Graduate Institute of Biomedical Electronics and Bioinformatics, National Taiwan University, Taipei 10617; [2]Taipei Beitou Health Management Hospital, Taipei 11252; [3]Philips Healthcare, Taipei 11503

Correspondence to: Hsiao-Wen Chung, PhD. Professor, Graduate Institute of Biomedical Electronics and Bioinformatics, National Taiwan University, Taipei 10617. Email: chunghw@ntu.edu.tw.

Background: To compare the depiction conspicuity of three-dimensional (3D) magnetic resonance cholangiopancreatography (MRCP) based on gradient- and spin-echo (GRASE) and two-dimensional (2D) thick-slab MRCP using fast spin-echo (FSE) in different segments of hepatic and pancreatic ducts at 3T.

Methods: Both 3D GRASE and 2D thick-slab FSE MRCP, with parameters adjusted under the constraints of specific absorption rate and scan time within single breath-hold, were performed for 95 subjects (M/F =49:46; age range, 25–75) at 3T. Conspicuity of eight ductal segments was graded by two experienced raters using a 4-point score. Situations where one technique is superior or inferior to the other were recorded.

Results: 3D GRASE MRCP outperformed 2D thick-slab FSE MRCP in the common bile duct and common hepatic ducts (both with P<0.001), but compared inferiorly in the right hepatic ducts (P<0.001), right posterior hepatic ducts (P<0.005) and pancreatic duct distal (P<0.05). Performing both 3D and 2D MRCP would reduce the number of non-diagnostic readings in the left hepatic duct to 10 remaining (5.3%), compared with 31 (16.3%) or 21 (11.1%) out of 190 readings if using 3D GRASE or 2D thick-slab FSE alone, respectively.

Conclusions: Although 3D GRASE MRCP is preferential to visualize the common bile duct and common hepatic duct within one single breath-hold, the complementary role of 2D thick-slab FSE MRCP in smaller hepatic and pancreatic ducts makes it a useful adjunct if performed additionally.

Keywords: Two-dimensional thick-slab acquisition (2D thick-slab acquisition); three-dimensional imaging (3D imaging); breath-hold; gradient- and spin-echo (GRASE); magnetic resonance cholangiopancreatography (MRCP)

Submitted Mar 03, 2020. Accepted for publication Apr 08, 2020.
doi: 10.21037/qims.2020.04.14
View this article at: http://dx.doi.org/10.21037/qims.2020.04.14

Introduction

The non-invasiveness of magnetic resonance cholangiopancreatography (MRCP) has long resulted in its preferential use in clinical practice over the invasive endoscopic retrograde cholangiopancreatography (ERCP) for first-line inspection (1,2). Although methods to obtain heavily T2-weighted MRCP images varied to some extent (3-5), fast spin-echo (FSE) remains the most widely employed technique in MRCP for its rapid scan and excellent immunity to susceptibility artifacts. The acquisition techniques for FSE-based MRCP could roughly be classified into two-dimensional (2D) and three-dimensional (3D) approaches (1,4). 2D thick-slab MRCP can be finished in a single excitation within seconds for

each slab (3,6). The major drawback is the lack of depth information to depict overlapping organs separately (4). On the other hand, multi-slice 2D thin-slice MRCP employs sequential acquisitions to acquire volumetric data, which lengthens the scan time and leads to inter-slice registration problems in the presence of subject motion (7). 3D MRCP is highly desirable in terms of spatial information, but its long scan time also causes respiratory motion to be non-negligible. Respiratory triggering (8) or navigator correction (9) is thus needed, however with residual motion artifacts inevitable for uncooperative patients.

If the total acquisition time can be reduced to about 15 seconds or less, 3D MRCP within one single breath-hold would be feasible. The simplest way to reduce scan time in FSE-based 3D MRCP is to shorten the echo spacing, at the expense of increased radiofrequency (RF) specific absorption rate (SAR) to the patients. Although not a severe problem at field strengths of 1.5 Tesla or lower, the SAR issue becomes critical at 3.0 Tesla or higher because power deposition scales more than linearly with the main field strength (10). One approach that may surrogate FSE in 3D MRCP is to insert a series of gradient echoes during each echo spacing interval in a way similar to echo-planar imaging (11), such that the amount of data obtained per single refocusing RF pulse can be increased. This method, termed the gradient- and spin-echo (GRASE) sequence (12,13), has recently been employed for 3D MRCP at 3.0 Tesla. Initial experience has documented successful 3D MRCP acquisition in 9–20 seconds under one single breath-hold, with image quality compared favorably to respiratory-triggered 3D FSE MRCP (14,15).

Despite of the obvious advantage of 3D GRASE for MRCP in terms of motion immunity as compared with 3D FSE at identical SAR, there are potential issues to be explored regarding this technique. Since GRASE is essentially a hybrid of gradient echo and FSE (11), susceptibility effects near air-tissue interfaces due to the gradient-echo nature (16) could possibly lead to undesired signal loss and hence may obscure particularly the pancreatic ducts. In addition, GRASE is known to exhibit point-spread-function-related blurring due to T2 and T2* decaying (17) which, along with matrix size settings within limited scan time, trades off the spatial resolution and could thus be detrimental for depicting small ducts. Furthermore, the scan time of 15 seconds is still considered long for patients who may not hold their breath perfectly. In this regard, the very fast 2D thick-slab MRCP technique based on conventional single-shot FSE may exhibit improved successful rate in uncooperative patients (3,6,7), and hence may still find its role as a useful adjunct to 3D GRASE MRCP. As a consequence, the purpose of this study is to compare the depiction conspicuity of 3D GRASE MRCP and 2D thick-slab FSE MRCP in eight different segments of hepatic and pancreatic ducts. Situations where one technique is superior or inferior to the other are examined and discussed, so as to investigate whether 3D GRASE is able to replace 2D thick-slab FSE for MRCP, or, to unravel the potential assisting role of 2D thick-slab FSE MRCP as an adjunct if 3D GRASE is set as the preferential protocol for routine MRCP examinations.

Methods

Subjects

This prospective study approved by our local institutional review board recruited 95 subjects (49 males, age 48.8±10.9 years, range, 25–75 years; 46 females, age 51.2±11.3 years, range, 25–73 years) between September 2018 and May 2019, from whom both 3D and 2D MRCP images were obtained. All subjects gave written informed consents before scanning, after explaining the purpose of this research to them. The subjects underwent magnetic resonance (MR) imaging of the gastrointestinal tract for the purpose of health examinations, and hence had no related symptoms at the time of imaging. No incidental findings regarding abnormality were identified from the MR images afterwards. Fasting for at least four hours was requested for all subjects before the examinations. No antiperistaltic agents were used, as these subjects were relatively healthy. Thus, the results from our study reflect imaging under natural conditions.

Image acquisition

In addition to routine gastrointestinal tract MR imaging sequences, MRCP was performed with both 3D GRASE and thick-slab 2D FSE techniques under instructed breath-hold before gadolinium contrast administration, if any. For 3D MRCP, images were acquired using the GRASE technique (14,15) with spectral adiabatic inversion recovery for fat suppression. A coronal volume (slightly oblique) with 60 mm thickness and 260×260 mm^2 field-of-view was prescribed. Five gradient echoes were inserted in each of the nine echo spacing intervals, corresponding to effective TE of 107 ms. TR was set to 262 ms to allow for some T1

recovery without prominently lengthening the total scan time. Matrix size was 172×169×50, resulting in acquisition voxel volume of 1.51×1.53×1.20 mm^3 reconstructed to 0.68×0.68×1.20 mm^3 with zero filling. The slice encoding direction was anterior-posterior. Frequency encoding direction was superior-inferior, and hence phase encoding was left-right. Parallel imaging acceleration factor was 3.7, leading to total scan time of 13.1 seconds. On the other hand, for 2D thick-slab MRCP, conventional single-shot FSE was used with oblique coronal orientation at 70 mm thickness and 256×256 mm^2 field-of-view [echo time/repetition time (TE/TR) =800/5,759 ms] to cover the entire biliary tree including the pancreas. Matrix size was 320×256 with full k-space coverage to yield acquisition voxel volume of 0.8×1.0×70 mm^3 reconstructed to 0.59×0.59×70 mm^3. No parallel imaging acceleration was used. The scan time, excluding preparation time needed to localize the slab, was 5.8 seconds per slab. The actual acquisition took 1.6 seconds to acquire at an echo spacing of 6.2 ms, with shortest TR of 5,759 ms set by the manufacturer for SAR restriction. The SAR levels estimated for both MRCP techniques were recorded from the operating console for all subjects before scanning to ensure maximization of acquisition efficiency within safety limits. Also note that since the scanning parameter settings were meant to generate the best image quality possible within one single breath hold, the single-shot 2D MRCP inherently allows a higher matrix size for better in-plane spatial resolution than 3D MRCP. In addition, because the purpose of this study was to explore the possible complementary value of 2D thick-slab FSE to assist 3D GRASE MRCP, 2D thick-slab FSE was prescribed after 3D GRASE acquisitions. No repeated examination was performed.

All imaging was done on a 3.0 Tesla system (Philips Ingenia) equipped with a 32-channel torso coil. One author (FM Chiu) was a Philips Healthcare employee and helped optimization of the scanning parameters during initial setup stage, but only the other authors had control on the performance evaluation and data analysis to minimize potential conflicts of interest.

Performance evaluation

Conspicuity of the hepatic and pancreatic ducts on the images was first assessed using image scoring by two board-certified readers. The reliability of the subjective image scoring, in turn, was then evaluated by performing inter-observer consistency test on the results from the two readers. Scoring of duct conspicuity was graded separately for the common bile duct (CBD), common hepatic duct (CHD), right hepatic duct (RHD), right anterior hepatic duct (RAD), right posterior hepatic duct (RPD), left hepatic duct (LHD), pancreatic duct proximal (PDP), and pancreatic duct distal (PDD), based on a 4-point conspicuity score, where 0 stands for not visible, 1 for visible but not of diagnostic quality, 2 for visible and of diagnostic quality, and 3 for excellent, respectively. Two board-certified radiologists (CP Chien and YC Shen) with 15 and 6 years of experience in abdominal radiology, respectively, read all the images, with inter-rater agreement assessed afterwards. The comparison was evaluated on the maximal intensity projection and free-rotating views from 3D MRCP (i.e., without referring to the original image slices) versus the 2D thick-slab MRCP images, bearing in mind that in reality 3D MRCP also allows retrospective examination of the original slices that cannot be achieved with 2D thick-slab MRCP. Due to distinct image appearance between 3D and 2D MRCP, it was impossible to blind the reading comparison.

Statistics

Inter-rater agreement was evaluated using Cohen's weighted kappa statistics. Wilcoxon signed rank test was used to compare the conspicuity scores for the eight ductal segments. Statistical significance was defined as $P<0.05$.

Results

The inter-rater agreements assessed separately for the eight ductal segments varied from 0.872 to 0.973, with overall agreement of 0.962, all by Cohen's weighted kappa. The very good inter-rater agreements suggest the conspicuity scores to be highly reliable, even if being somewhat subjective. *Figure 1* summarizes the mean conspicuity scores for 3D GRASE and 2D thick-slab FSE MRCP. 3D GRASE MRCP was found to be diagnostically useful for most subjects (mean scores >2) for CBD (2.74±0.50), CHD (2.81±0.46), RHD (2.09±0.94), and LHD (2.23±0.77), whereas 2D thick-slab FSE MRCP showed similar findings (2.29±0.99 for CHD, 2.08±0.91 for RHD, and 2.27±0.67 for LHD, respectively) except that it failed to provide diagnostic value for CBD in the majority of subjects (mean scores 1.35±0.95). For RAD, RPD, PDP, and PDD, neither MRCP methods investigated in this study were diagnostically helpful in most of the recruited subjects (mean scores <2). 3D GRASE MRCP outperformed 2D thick-slab

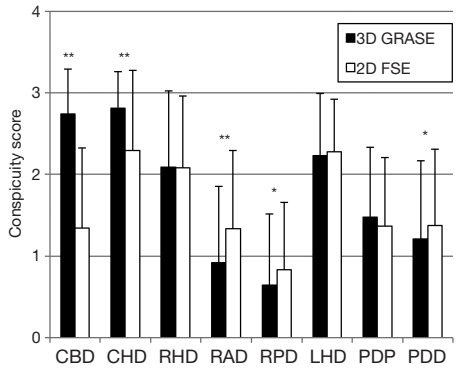

Figure 1 Mean conspicuity scores for the eight ductal segments evaluated for MRCP acquired using 3D GRASE (filled bars) and thick-slab 2D FSE (open bars). Error bars are standard deviations of 190 readings from 95 subjects. Asterisks stand for statistically significant difference (*, P<0.05; **, P<0.001). CBD, common bile duct; CHD, common hepatic duct; RHD, right hepatic duct; RAD, right anterior hepatic duct, RPD, right posterior hepatic duct; LHD, left hepatic duct; PDP, pancreatic duct proximal; PDD, pancreatic duct distal; 2D FSE, two-dimensional thick-slab fast spin-echo; 3D GRASE, three-dimensional gradient- and spin-echo.

FSE MRCP in CBD and CHD (2.74±0.50 *vs.* 1.35±0.95 for CBD and 2.81±0.46 *vs.* 2.29±0.99 for CHD, respectively, both with P<0.001; *Figures 2,3*), but compared inferiorly in RAD (0.92±0.93 *vs.* 1.34±0.93, P<0.001; *Figure 2*), RPD (0.65±0.88 *vs.* 0.84±0.81, P<0.005), and PDD (1.21±0.96 *vs.* 1.38±0.93, P<0.05). For RHD, LHD, and PDP, differences between the two MRCP techniques were statistically insignificant (P>0.05).

In addition to the grouped results in *Figure 1*, comparisons of conspicuity on an individual basis are also listed in *Tables 1-3* for RHD, LHD, and PDP, respectively, the three ducts that showed statistically insignificant differences between 3D GRASE and 2D thick-slab FSE MRCP. Note in these tables that all nonzero entries falling on the diagonal line would mean that 3D GRASE and 2D thick-slab FSE provided exactly equal value in MRCP. In contrast, presence of nonzero numbers in off-diagonal entries would suggest mutually complementary value, where the lower-left corner means that 3D GRASE helps remedy the inadequacy of 2D thick-slab FSE, and vice versa for the upper-right corner. Note in particular *Table 2* for LHD. Although results from *Figure 1* indicated that 3D GRASE

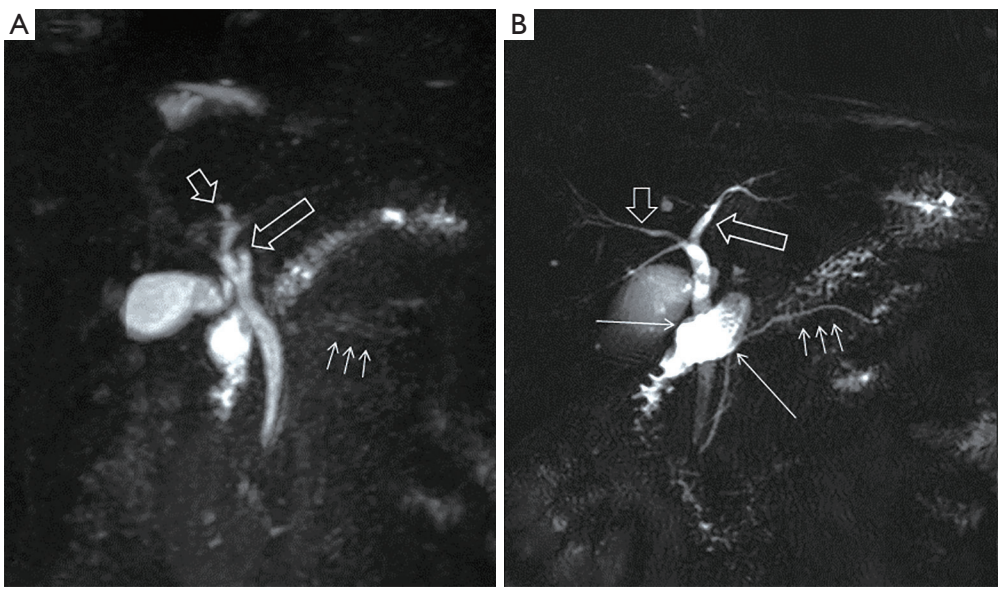

Figure 2 Comparison on conspicuity between 3D GRASE and 2D thick-slab FSE MRCP. (A) The availability of volumetric data in 3D GRASE MRCP from the 52-year-old female subject allows free rotation of the entire slab such that both the common bile duct and the common hepatic duct are clearly visualized with diagnostic quality. The left (long open arrow) and right hepatic ducts (short open arrow) and the pancreatic duct (short arrows), however, are not visualized. (B) In 2D MRCP, although the duodenum fluid obscures part of the common bile duct (long arrows), the left and right hepatic ducts (open arrows) and the pancreatic duct (short arrows) are better visualized than on 3D MRCP, likely due to superior in-plane resolution. 2D, two dimensional; 3D, three-dimensional; FSE, fast spin-echo; GRASE, gradient- and spin-echo; MRCP, magnetic resonance cholangiopancreatography.

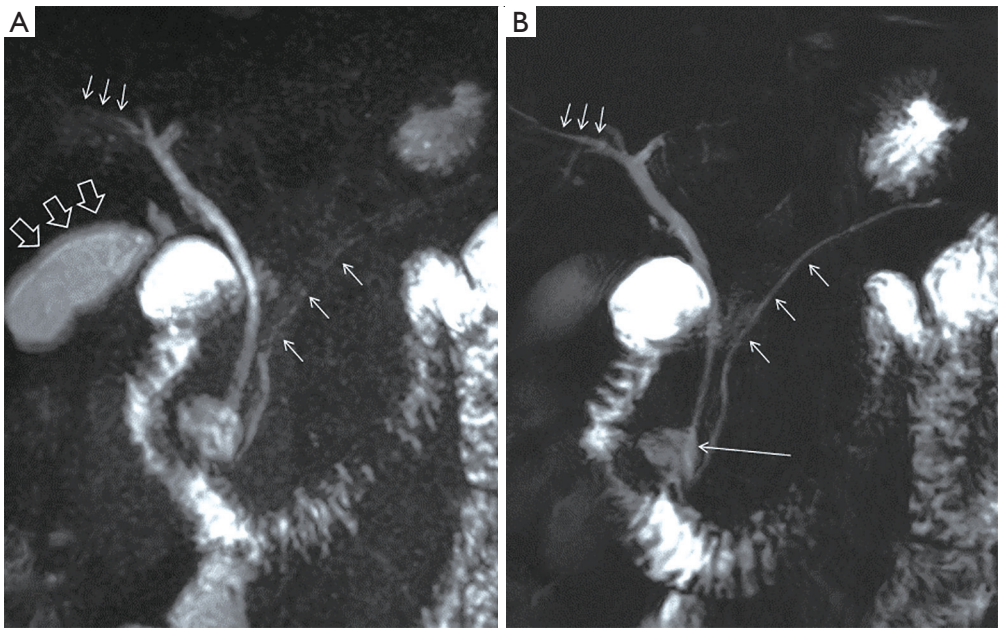

Figure 3 Comparison on conspicuity between 3D GRASE and 2D thick-slab FSE MRCP. (A) Blurring arising from residual motion of the 66-year-old male subject (open arrows) is clearly seen in the 3D MRCP projection image even if breath holding was considered largely successful. Identification of the right hepatic duct and the pancreatic duct distal (short arrows) is hampered. On the other hand, the opening of the common bile duct could be identified from the source images retrospectively in this case. (B) In comparison, motion freezing from the short scan time as well as high in-plane spatial resolution of 2D MRCP is beneficial for the depiction of right hepatic duct and the pancreatic duct distal (short arrows). Depiction of common bile duct opening was however suboptimal in 2D MRCP due to obstruction by the presence of fluid in the juxtapapillary diverticulum (long arrow). 2D, two dimensional; 3D, three-dimensional; FSE, fast spin-echo; GRASE, gradient- and spin-echo; MRCP, magnetic resonance cholangiopancreatography.

Table 1 Conspicuity score distribution for the right hepatic duct

3D GRASE	2D FSE				
	0	1	2	3	Sub-total
0	5	3	3	1	12
1	3	24	9	4	40
2	2	6	32	17	57
3	1	5	22	53	81
Sub-total	11	38	66	75	190

2D FSE, two-dimensional thick-slab fast spin-echo; 3D GRASE, three-dimensional gradient- and spin-echo.

Table 2 Conspicuity score distribution for the left hepatic duct

3D GRASE	2D FSE				
	0	1	2	3	Sub-total
0	0	0	2	2	4
1	1	9	15	2	27
2	0	6	47	28	81
3	0	5	31	42	78
Sub-total	1	20	95	74	190

2D FSE, two-dimensional thick-slab fast spin-echo; 3D GRASE, three-dimensional gradient- and spin-echo.

and 2D thick-slab FSE MRCP were not statistically different in terms of LHD depiction, there were a prominent portion of readings (92 out of 190; 48.4%) falling in the off-diagonal entries, with both upper-left and lower-right entries found. In particular, 3D GRASE alone would miss reliable diagnosis (score =0 or 1) in 31 readings (16.3%; upper-right corner subtotal 4+27 in *Table 2*) (*Figure 2*), whereas 2D thick-slab FSE would miss 21 (11.1%; lower-left corner subtotal 1+20 in *Table 2*) (*Figure 4*). Performing both 3D and 2D acquisitions would reduce the non-diagnostic readings to only 10 remaining (5.3%; four elements at the upper-left corner 0+0+1+9 in *Table 2*). Data

from RHD (*Table 1*) and PDP (*Table 3*) demonstrated trends similar to LHD for the mutually complementary roles of 3D GRASE and 2D thick-slab FSE for MRCP. For the other five ducts where 3D GRASE and 2D thick-slab FSE exhibited statistically significant difference in conspicuity, the mutually complementary roles are still seen, albeit not as prominent as in RHD, LHD, and PDP (not shown).

Discussion

The replacement of highly invasive ERCP by noninvasive MRCP for first-line inspection of the biliary tree relies on the important prerequisite of accurate depiction of various ducts in MRCP (18). Consequently, image quality and duct conspicuity in MRCP are both critically important aspects (19). The superiority of 3D GRASE for MRCP over the respiratory-triggered 3D FSE reported by independent investigators gives some hope in successful breath holding to overcome the respiratory motion (14,15). However, comparative effectiveness between 3D GRASE and 2D thick-slab FSE MRCP has not been documented in detail, to the best of our knowledge. It is for this reason that we conducted this study on a fairly large cohort of subjects. Results from our study suggest that, under the constraint of limited scan time within single breath-hold, settings of scanning parameters in 3D GRASE MRCP within SAR safety limits at 3.0 Tesla resulted in trade-off in various aspects such as in-plane spatial resolution (15). Hence, although the availability of free rotation of the 3D data helped better visualization of CBD and CHD (14,15), depiction of RAD, RPD, and PDD was hampered in comparison with 2D thick-slab FSE MRCP. For RHD, LHD, and PDP, the two MRCP methods investigated in our study provided complementary value and should thus ideally be both performed. In other words, the clinical significance of our study is that we have provided evidence on the recommendation of routine protocol settings in

Table 3 Conspicuity score distribution for the pancreatic duct proximal

3D GRASE	2D FSE				
	0	1	2	3	Sub-total
0	6	13	3	0	22
1	12	39	21	3	75
2	8	25	38	2	73
3	0	4	8	8	20
Sub-total	26	81	70	13	190

2D FSE, two-dimensional thick-slab fast spin-echo; 3D GRASE, three-dimensional gradient- and spin-echo.

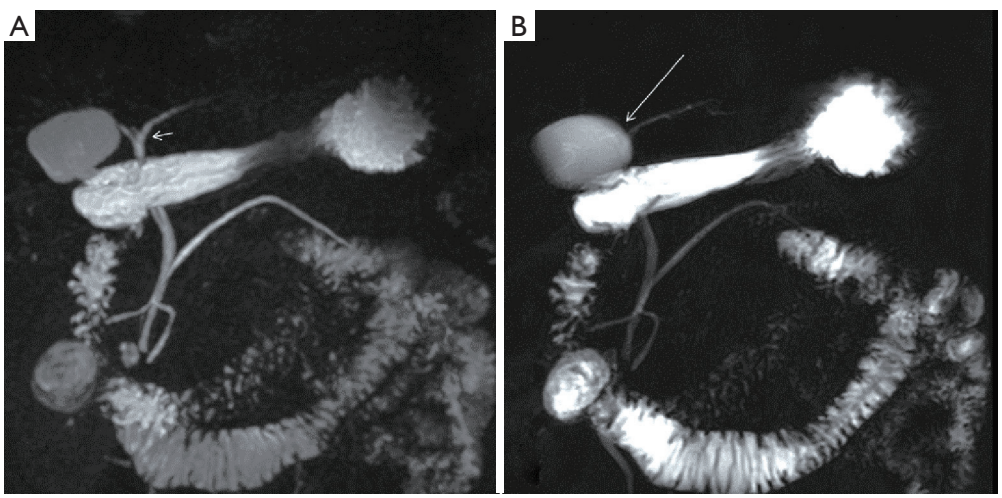

Figure 4 Comparison on conspicuity between 3D GRASE and 2D thick-slab FSE MRCP. Images from the 46-year-old male subject showing better visualization of the left hepatic duct on 3D GRASE MRCP than on 2D thick-slab FSE MRCP. (A) In this subject, the relatively high location of the duodenum bulb results in its close proximity to the opening of the left hepatic duct. Identification of the left hepatic duct opening (short arrow) on 3D MRCP could be achieved via free rotation of the projection view. (B) 2D MRCP suffers from signal overlapping with the duodenum bulb (long arrow), hampering visualization of the opening of left hepatic duct. 2D, two dimensional; 3D, three-dimensional; FSE, fast spin-echo; GRASE, gradient- and spin-echo; MRCP, magnetic resonance cholangiopancreatography.

abdominal MR examination at 3.0 Tesla, namely the inclusion of 2D thick-slab FSE as an adjunct to 3D GRASE for MRCP.

Reasons for the comparative effectiveness of 3D GRASE MRCP versus 2D thick-slab FSE MRCP could be appreciated from the characteristics of the ductal anatomy as well as technical properties in MR. For CBD and CHD, the two major biliary ducts where most pathologies such as stone or obstruction are found (6), the sufficiently large diameters (about 5–6 mm) are in favor of 3D GRASE MRCP which has lower in-plane spatial resolution than 2D thick-slab FSE MRCP in our protocol settings (14). In particular for CBD, 2D thick-slab FSE MRCP suffered from signal overlapping with residual fluid in the duodenum (19). Unlike 3D MRCP where retrospective viewing from different angles is allowed to depict CBD, 2D thick-slab MRCP is restricted to the orientations of the acquisition slabs. In other words, once the 2D scan is finished, the chance to avoid duodenum overlapping with CBD is lost. Although increasing the number of rotating slabs for 2D MRCP prescription may help resolving the issue of overlapping (3,6), this is achieved at the expense of substantially increased scan time because of TR lengthening to allow for T1 recovery as well as to restrict SAR (1). 3D GRASE thus seems to be preferable for CBD and CHD compared with 2D thick-slab FSE for MRCP.

Inferiority of 3D GRASE to 2D thick-slab FSE MRCP in RAD, RPD, and PDD is attributed to difference in in-plane spatial resolution because of the small size of these ducts (15). Despite that the voxel volume of $1.51\times1.53\times1.20$ mm^3 in 3D GRASE MRCP was theoretically adequate in resolving these ducts, the actual spatial resolution could easily be impeded by residual subject motion and point-spread-function blurring (11,17). Here the very short scan time of 2D thick-slab FSE MRCP plus its high in-plane resolution provided important advantage for depiction of small ducts compared with 3D GRASE MRCP.

Even if the comparative effectiveness reported in our study looks straightforward, interpretation of the statistical results should be exercised with caution. Specifically, when statistically significant difference is absent between 3D GRASE and 2D thick-slab FSE MRCP, two possibilities have to be considered. One extreme is that the two methods are equally effective, and the other is that 3D GRASE and 2D thick-slab FSE MRCP complement each other under different situations. At least in the case of LHD, our data indicate that LHD depiction would benefit from both 3D GRASE and 2D thick-slab FSE MRCP, suggesting that ideally 3D GRASE and 2D thick-slab MRCP should both be used to increase successful depiction. Similarly, for RHD, RAD, RPD, PDP, and PDD, the complementary role of 2D thick-slab FSE MRCP should not be ignored because visualization of these ducts with 3D GRASE could be hindered by inadequate in-plane resolution, susceptibility-related signal loss (16), or residual patient motion, all being relatively disadvantageous in 3D GRASE MRCP.

Signal overlapping with duodenum fluid, an important disadvantage of 2D thick-slab FSE MRCP for CBD, can be effectively remedied by applying natural negative oral contrast agent such as pineapple juice (20). In our study, oral contrast agent was not used because the metal ion contents are known to shorten both T1 and T2 (21). Since the TR of 262 ms chosen for 3D GRASE MRCP resulted in prominent T1 weighting as opposed to the long TR of 5,759 ms in 2D thick-slab FSE, using oral contrast would favor 2D thick-slab FSE by suppressing signals from the gastrointestinal tract, but may hurdle 3D GRASE for MRCP from increased background signals. For the same reason, in clinical practice if natural negative oral contrast were to be used, administration after 3D GRASE acquisition but before 2D FSE for MRCP would be recommended.

There are several limitations in this study. The cohort, due to the nature of our affiliations, was from subjects undergoing imaging health examinations who had no pathology and were largely cooperative. As a result, evaluation of the conspicuity score was unproven in the presence of abnormalities (9). In addition, the subject motion issue encountered in our study should be regarded as the best-case scenario somewhat favoring the longer scan time for 3D GRASE MRCP. In clinical routine where the patients may have difficulty maintaining instructed breath-hold, success rate alone would somehow favor 2D MRCP, because the scan time of 13.1 seconds for 3D GRASE MRCP, even if generally regarded as tolerable for most patients, is still substantially longer than that for 2D thick-slab FSE MRCP per slab. Under these specific situations, respiratory-triggered (22,23) or free-breathing (9,24) 3D MRCP should be chosen in replacement of breath-holding 3D GRASE. The complementary value of 2D thick-slab FSE to respiratory-triggered 3D sequences for MRCP is similar to the findings from our study, as documented in previous works (22,23). A second limitation more on the technical aspect is that we did not compare 3D MRCP acceleration using other approaches, such as compressed sensing (25,26), balanced steady-state free precession (5),

or fast-recovery FSE (4,27). Compressed sensing is purely a reconstruction algorithm for randomized undersampling of the phase encoding steps, hence is fully compatible with 3D GRASE MRCP (26). On the other hand, balanced steady-state free precession and fast-recovery FSE are two different readout design alternatives to GRASE, probably promoted by different manufacturers and thus hard to compare under the same system platform. In fact, to our knowledge, 3D GRASE so far does not seem to be widely employed for MRCP by other manufacturers (11). Nevertheless, balanced steady-state free precession is known to exhibit banding artifacts particularly prominent at high fields (28), whereas fast-recovery FSE exhibiting exactly the same SAR issue as 3D FSE might restrict MRCP applications to field strengths of 1.5 Tesla or lower (4,27). Therefore, it is anticipated that 2D thick-slab FSE MRCP would also likely provide complementary value to the above 3D alternatives at 3.0 Tesla, although this remains to be investigated.

Conclusions

We conclude that although 3D GRASE MRCP is the preferential choice to depict CBD and CHD with depth information at freely viewing angles, the complementary role of 2D thick-slab FSE MRCP in other smaller hepatic and pancreatic ducts makes it a useful adjunct if performed additionally during routine examinations. Both methods allow MRCP to be acquired within one single breath-hold to reduce negative impact from subject motions.

Acknowledgments

Funding: HWC received support in part from the Ministry of Science and Technology under grants MOST 105-2221-E-002-142-MY3 and MOST 107-2221-E-002-038-MY3.

Footnote

Conflicts of Interest: All authors have completed the ICMJE uniform disclosure form (available at http://dx.doi.org/10.21037/qims.2020.04.14). FMC reports employment at Philips Healthcare, Taipei. HWC reports grants and personal fees from Ministry of Science and Technology during the conduct of the study; plus personal fees from Taipei Medical University Hospital, Tri-Service General Hospital, and Chi-Mei Hospital outside the submitted work. HWC serves as an unpaid editorial board member of *Quantitative Imaging in Medicine and Surgery*. The other authors have no conflicts of interest to declare.

Ethical Statement: This prospective study was approved by our local institutional review board. All subjects gave written informed consents before scanning, after explaining the purpose of this research to them.

References

1. Becker CD, Grossholz M, Mentha G, de Peyer R, Terrier F. MR cholangiopancreatography: technique, potential indications, and diagnostic features of benign, postoperative, and malignant conditions. Eur Radiol 1997;7:865-74.
2. Takehara Y. Can MRCP replace ERCP? J Magn Reson Imaging 1998;8:517-34.
3. Vitellas KM, Keogan MT, Spritzer CE, Nelson RC. MR cholangiopancreatography of bile and pancreatic duct abnormalities with emphasis on the single-shot fast spin-echo technique. Radiographics 2000;20:939-57.
4. Sodickson A, Mortele KJ, Barish MA, Zou KH, Thibodeau S, Tempany CM. Three-dimensional fast-recovery fast spin-echo MRCP: comparison with two-dimensional single-shot fast spin-echo techniques. Radiology 2006;238:549-59.
5. Glockner JF, Saranathan M, Bayram E, Lee CU. Breath-held MR cholangiopancreatography (MRCP) using a 3D Dixon fat-water separated balanced steady state free precession sequence. Magn Reson Imaging 2013;31:1263-70.
6. Fulcher AS, Turner MA, Capps GW, Zfass AM, Baker KM. Half-Fourier RARE MR cholangiopancreatography: experience in 300 subjects. Radiology 1998;207:21-32.
7. Yamashita Y, Abe Y, Tang Y, Urata J, Sumi S, Takahashi M. In vitro and clinical studies of image acquisition in breath-hold MR cholangiopancreatography: single-shot projection technique versus multislice technique. AJR Am J Roentgenol 1997;168:1449-54.

8. Textor HJ, Flacke S, Pauleit D, Keller E, Neubrand M, Terjung B, Gieseke J, Scheurlen C, Sauerbruch T, Schild HH. Three-dimensional magnetic resonance cholangiopancreatography with respiratory triggering in the diagnosis of primary sclerosing cholangitis: comparison with endoscopic retrograde cholangiography. Endoscopy 2002;34:984-90.
9. Morita S, Ueno E, Suzuki K, Machida H, Fujimura M, Kojima S, Hirata M, Ohnishi T, Imura C. Navigator-triggered prospective acquisition correction (PACE) technique vs. conventional respiratory-triggered technique for free-breathing 3D MRCP: an initial prospective comparative study using healthy volunteers. J Magn Reson Imaging 2008;28:673-7.
10. Hand JW, Lagendijk JJ, Hajnal JV, Lau RW, Young IR. SAR and temperature changes in the leg due to an RF decoupling coil at frequencies between 64 and 213 MHz. J Magn Reson Imaging 2000;12:68-74.
11. Chu ML, Chien CP, Wu WC, Chung HW. Gradient- and spin-echo (GRASE) MR imaging: a long-existing technology that may find wide applications in modern era. Quant Imaging Med Surg 2019;9:1477-84.
12. Oshio K, Feinberg DA. GRASE (Gradient- and spin-echo) imaging: a novel fast MRI technique. Magn Reson Med 1991;20:344-9.
13. Feinberg DA, Oshio K. GRASE (gradient- and spin-echo) MR imaging: a new fast clinical imaging technique. Radiology 1991;181:597-602.
14. Yoshida M, Nakaura T, Inoue T, Tanoue S, Takada S, Utsunomiya D, Tsumagari S, Harada K, Yamashita Y. Magnetic resonance cholangiopancreatography with GRASE sequence at 3.0T: does it improve image quality and acquisition time as compared with 3D TSE? Eur Radiol 2018;28:2436-43.
15. Nam JG, Lee JM, Kang HJ, Lee SM, Kim E, Peeters JM, Yoon JH. GRASE revisited: breath-hold three-dimensional (3D) magnetic resonance cholangiopancreatography using a Gradient and Spin Echo (GRASE) technique at 3T. Eur Radiol 2018;28:3721-8.
16. Mugler JP 3rd, Brookeman JR. Off-resonance image artifacts in interleaved-EPI and GRASE pulse sequences. Magn Reson Med 1996;36:306-13.
17. Johnson G, Feinberg DA, Venkataraman V. A comparison of phase encoding ordering schemes in T2-weighted GRASE imaging. Magn Reson Med 1996;36:427-35.
18. Jenkins JT, Glass G, Ballantyne S, Fullarton GM. Effect of MRCP introduction on ERCP practice: are there implications for service and training? Gut 2006;55:1365-6.
19. Irie H, Honda H, Kuroiwa T, Yoshimitsu K, Aibe H, Shinozaki K, Masuda K. Pitfalls in MR cholangiopancreatographic interpretation. Radiographics 2001;21:23-37.
20. Riordan RD, Khonsari M, Jeffries J, Maskell GF, Cook PG. Pineapple juice as a negative oral contrast agent in magnetic resonance cholangiopancreatography: a preliminary evaluation. Br J Radiol 2004;77:991-9.
21. Espinosa MG, Sosa M, De León-Rodríguez LM, Córdova T, Bernal-Alvarado J, Avila-Rodríguez M, Reyes-Aguilera JA, Ortíz JJ, Barrios FA. Blackberry (Rubus spp.): a pH-dependent oral contrast medium for gastrointestinal tract images by magnetic resonance imaging. Magn Reson Imaging 2006;24:195-200.
22. Chavhan GB, Almehdar A, Moineddin R, Gupta S, Babyn PS. Comparison of respiratory-triggered 3-D fast spin-echo and single-shot fast spin-echo radial slab MR cholangiopancreatography images in children. Pediatr Radiol 2013;43:1086-92.
23. Masui T, Katayama M, Kobayashi S, Nozaki A, Sugimura M, Ikeda M, Sakahara H. Magnetic resonance cholangiopancreatography: comparison of respiratory-triggered three-dimensional fast-recovery fast spin-echo with parallel imaging technique and breath-hold half-Fourier two-dimensional single-shot fast spin-echo technique. Radiat Med 2006;24:202-9.
24. Zhang J, Israel GM, Hecht EM, Krinsky GA, Babb JS, Lee VS. Isotropic 3D T2-weighted MR cholangiopancreatography with parallel imaging: feasibility study. AJR Am J Roentgenol 2006;187:1564-70.
25. Lohöfer FK, Kaissis GA, Rasper M, Katemann C, Hock A, Peeters JM, Schlag C, Rummeny EJ, Karampinos D, Braren RF. Magnetic resonance cholangiopancreatography at 3 Tesla: Image quality comparison between 3D compressed sensing and 2D single-shot acquisitions. Eur J Radiol 2019;115:53-8.
26. Zhu L, Xue H, Sun Z, Qian T, Weiland E, Kuehn B, Asbach P, Hamm B, Jin Z. Modified breath-hold compressed-sensing 3D MR cholangiopancreatography with a small field-of-view and high resolution acquisition: clinical feasibility in biliary and pancreatic disorders. J Magn Reson Imaging 2018;48:1389-99.
27. Nandalur KR, Hussain HK, Weadock WJ, Wamsteker EJ, Johnson TD, Khan AS, D'Amico AR, Ford MK, Nandalur SR, Chenevert TL. Possible biliary disease: diagnostic performance of high-spatial-resolution isotropic 3D T2-weighted MRCP. Radiology 2008;249:883-90.

28. Chung HW, Chen CY, Zimmerman RA, Lee KW, Lee CC, Chin SC. T2-Weighted fast MR imaging with true FISP versus HASTE: comparative efficacy in the evaluation of normal fetal brain maturation. AJR Am J Roentgenol 2000;175:1375-80.

Cite this article as: Chien CP, Chiu FM, Shen YC, Chen YH, Chung HW. Magnetic resonance cholangiopancreatography at 3T in a single breath-hold: comparative effectiveness between three-dimensional (3D) gradient- and spin-echo and two-dimensional (2D) thick-slab fast spin-echo acquisitions. Quant Imaging Med Surg 2020;10(6):1265-1274. doi: 10.21037/qims.2020.04.14

